Nonlinear tunneling in a fiber guide array resonator

Jérôme Leon
Physique Mathématique et Théorique, CNRS-UMR5825 Université Montpellier 2, 34095 Montpellier, France
(Received 27 February 2004; revised manuscript received 9 August 2004; published 15 November 2004)

A fiber guide array resonator is proposed and shown to obey a nonlinear Schrödinger model in a square well potential with nonlinearity defocusing inside the well and focusing outside. This model is proved to possess nonlinear states which are i) continuous extensions of the linear eigenstates, ii) remarkably stable up to a threshold amplitude, iii) unstable at the threshold where *nonlinear tunneling* occurs by gap soliton emission outside the well. This allows in particular to obtain soliton formation by constant wave irradiation of the fiber guide array resonator. An explicit analytic expression of the threshold is given in terms of the well size for each level.

DOI: 10.1103/PhysRevE.70.056604 PACS number(s): 05.45.Yv, 42.65.Tg

INTRODUCTION

Fiber guide arrays have attracted much attention because of their extremely rich optical properties resulting from power exchange betwen adjacent waveguides [1]. Such a *directional coupling* induces anomalous refraction and diffraction [2].

Those devices can be worked out in the nonlinear (Kerr) regime and acquire then strikingly unusual properties such as self-modulation for soliton generation [3], experimentally demonstrated in [4], Floquet-Bloch solitons reported in [5], discrete stationary gap solitons experimentally observed in [6], and unusual beam propagation properties discussed (theoretically and experimentally) in [7]. Lastly, a recent proposal [8] is to generate *discrete gap solitons* by boundary driving a fiber guide array *above the cutoff*, an approach that uses the theory of nonlinear supratransmission [9].

We consider here a fiber array in the nonlinear Kerr regime [10] when different types of fibers are used: a self-focusing medium with dielectric constant ϵ_1 confines a self-defocusing medium with $\epsilon_2 > \epsilon_1$, as sketched in Fig. 1. The injected radiation (shown by the arrows) can be tuned to a frequency in the forbidden band of the outside medium that acts then as a Bragg mirror for the tranverse modulation. This constitutes our *fiber guide array resonator*.

Following [3], the propagation of laser irradiation along the direction t is governed by the discrete nonlinear Schrödinger equation (NLS) for the envelopes $\psi(n,t)$ of the fiber modes. In the continuous limit (large number of fibers and weak coupling), it results as the following model ($x = nd$ where d is the array spacing):

$$i\psi_t + \psi_{xx} + |\psi|^2\psi = V\psi, \quad |x| > L,$$

$$i\psi_t + \psi_{xx} - |\psi|^2\psi = 0, \quad |x| < L \tag{1}$$

that has *repulsive* self-interaction inside the well and *attractive* outside. The positive constant V is the well height proportional to the dielectric constant difference $\epsilon_2 - \epsilon_1$, and $2L$ is its width.

Although the physical situation related to the device of Fig. 1 is that of a discrete system, using the continuous model above allows us to derive explicit solutions and to study them in detail. We will report in future studies on the fully discrete case and we note that the continuous model is of wide applicability as a generic nonlinear Schrödinger equation in a squared potential well.

The nonlinear states for NLS with a definite sign of the nonlinearity have been derived in [11] with interesting solutions having no counterparts in the linear limit. Using different nonlinearities as in Eq. (1) actually allows us to obtain a system whose nonlinear state solutions possess remarkable properties: (i) they uniformly tend to the linear eigenstates in the small-amplitude limit, (ii) they are stable solutions for amplitudes below an explicit threshold, and (iii) at threshold amplitude, an instability generates gap solitons, emitted outside the well, hence realizing a classical nonlinear tunneling process.

The threshold values will be explicitely calculated for the entire set of nonlinear states in terms of the well height V and eigenfrequencies in formula (18) below. We shall also demonstrate that the small-amplitude limit maps continuously the nonlinear states to the linear ones.

The fiber guide array resonator then appears as a means to generate gap solitons by constant wave (CW) input radiation at a flux intensity given explicitly in terms of the dimensions of the dielectric constant variation $\epsilon_2 - \epsilon_1$. Figure 2 displays a typical numerical simulation of Eq. (1) that shows the evolution of the fundamental mode at the threshold for which the input envelope is indeed CW-like and experiences an instability generating the gap soliton.

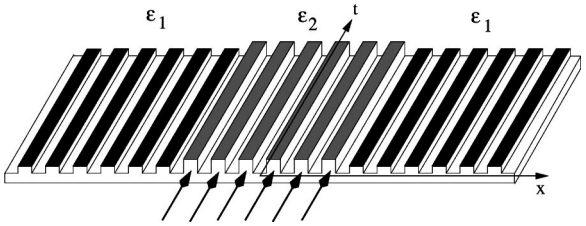

FIG. 1. Sketch of the fiber guide array resonator. The dimensionless propagation direction is denoted by the variable t, the transverse (dimensionless) direction is the variable x. The arrows indicate the injected radiation.

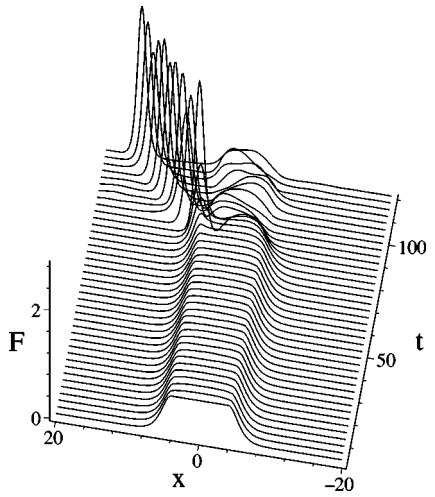

FIG. 2. Evolution of the flux density $F=|\psi|^2$ for the fundamental zero-mode initial datum at threshold amplitude in the case $V=1$ and $L=4$. The analytic expression of the input is given by expressions (4) and (13) at $t=0$ for modulus μ and amplitude A given in Eq. (21). The solution inside the well here is simply the constant $A_s=\sqrt{2V/3}$.

NONLINEAR STATES

We first need to recall the linear eigenstates that read in the odd case

$$\psi=\begin{cases} Ae^{-i\omega t}\sin(kx), & |x|\leqslant L \\ Ae^{-i\omega t}\sin(kL)e^{-\kappa(|x|-L)}, & |x|\geqslant L, \end{cases}$$

$$k^2=V\sin^2(kL), \quad \tan(kL)<0, \tag{2}$$

and in the even case

$$\psi=\begin{cases} Ae^{-i\omega t}\cos(kx), & |x|\leqslant L \\ Ae^{-i\omega t}\cos(kL)e^{-\kappa(|x|-L)}, & |x|\geqslant L, \end{cases}$$

$$k^2=V\cos^2(kL), \quad \tan(kL)>0, \tag{3}$$

for $\omega=k^2<V$ and $\kappa^2=V-\omega$, and for arbitrary amplitude A.

As learned from [11], the main tool to derive the nonlinear states is to connect a periodic solution inside the well to a static one-soliton tail outside. We make use of the fundamental solutions of NLS in terms of Jacobi elliptic functions for both symmetric (even) and antisymmetric (odd) cases [12]. First, outside the potential well we have the common soliton tails

$$\psi=\frac{\kappa\sqrt{2}e^{-i\omega t}}{\cosh[\kappa(|x|-L+d)]}, \quad |x|\geqslant L, \quad \kappa^2=V-\omega, \tag{4}$$

which replaces the two evanescent waves of the linear case. Inside the well, the basic stationary solution reads

$$\psi=\mu Ae^{-i\omega t}\mathrm{sn}(A'x+x_0,\mu), \quad |x|\leqslant L. \tag{5}$$

Here and in the following, the *amplitude A* is real-valued and positive and we define the new constant A' by $A=A'\sqrt{2}$. Odd and even solutions will be obtained by convenient choices of x_0.

Expression (5) is a solution of Eq. (1) if (necessary condition)

$$\omega^2=\frac{1}{2}A^2(1+\mu^2), \tag{6}$$

which links the frequency ω to the modulus μ of the elliptic functions. The requirement $\omega<V$ for a bound state implies that the modulus μ cannot exceed the following maximum value μ_m:

$$\mu\leqslant(2V/A^2-1)^{1/2}=\mu_m. \tag{7}$$

We discovered that it is necessary to work with expressions of the solution for moduli $\mu>1$, performed by means of the identity $\mu\,\mathrm{sn}(\mathrm{u},\,\mu)=\mathrm{sn}(\mu\mathrm{u},\,1/\mu)$.

ODD SOLUTIONS

In the range $\mu\in[1,\,\mu_m]$ we define with $x_0=0$ the following solution inside the well:

$$\psi=Ae^{-i\omega t}sn\left(\mu A'x,\,\frac{1}{\mu}\right), \quad |x|\leqslant L. \tag{8}$$

In order to obtain sufficient conditions for the set (8) and (4) to be a solution of Eq. (1), we require continuity of the solution and its derivative in $x=\pm L$. This provides the admissible discrete set of moduli μ which, after some algebra, must solve

$$\mu^2cn^2\left(b,\frac{1}{\mu}\right)dn^2\left(b,\frac{1}{\mu}\right)=sn^2\left(b,\frac{1}{\mu}\right)\left[\frac{2V}{A^2}-(1+\mu^2)-sn^2\left(b,\frac{1}{\mu}\right)\right], \tag{9}$$

where the function b is defined as

$$b=\mu A'L. \tag{10}$$

Then the shift d of the tail position for each solution μ of the above equation is given by

$$A\left|sn\left(b,\frac{1}{\mu}\right)\right|=\frac{\kappa\sqrt{2}}{\cosh(\kappa d)}. \tag{11}$$

As for the linear case, one must add a consistency condition for the signs of the derivatives. It is just a matter of careful reading of all possible cases to obtain the condition

$$sn\left(b,\frac{1}{\mu}\right)cn\left(b,\frac{1}{\mu}\right)dn\left(b,\frac{1}{\mu}\right)<0 \tag{12}$$

for the solution μ of Eq. (9) to be acceptable.

EVEN SOLUTIONS

Still with $\mu\in[1,\mu_m]$, we define

$$\psi=Ae^{-i\omega t}sn\left(\mu A'x+K\left(\frac{1}{\mu}\right),\frac{1}{\mu}\right), \quad |x|<L \tag{13}$$

obtained from Eq. (5) by the translation $x_0=K(1/\mu)/\mu$, where K is the complete elliptic integral of the first kind. In

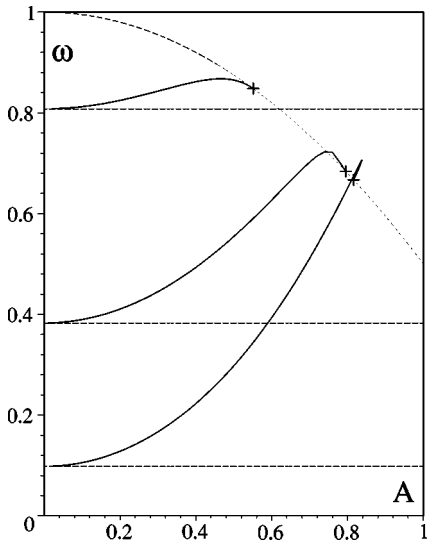

FIG. 3. Dependence of the eigenvalues ω in terms of the amplitude for $V=1$ and $L=4$. Crosses indicate the values of amplitude threshold and the dashed curve is the prediction of global threshold (18).

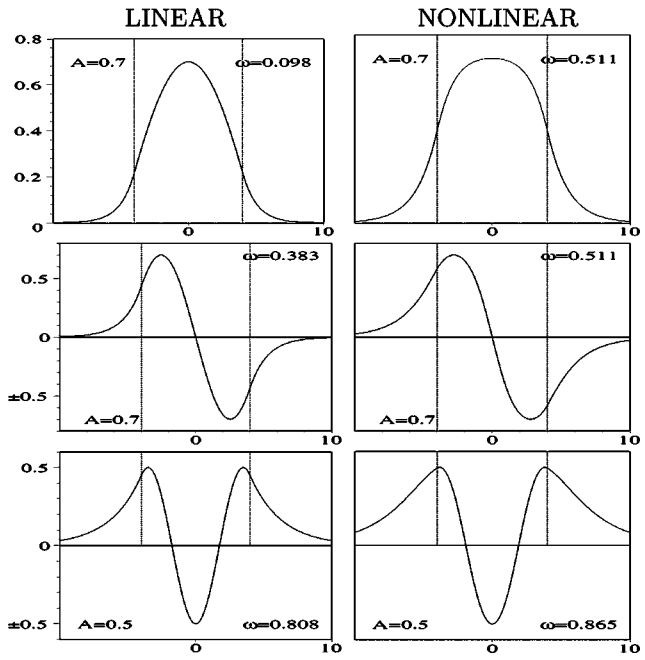

FIG. 4. Plots of the nonlinear states (8) and (13) (right) at $t=0$ as functions of the transverse variable x (with $V=1$ and $L=4$) compared to the linear ones given in Eqs. (2) and (3) (left), with amplitudes and frequencies as indicated. The same vertical scale is used for linear and nonlinear figures, the horizontal axis is the transverse x variable.

that case, the continuity conditions give the admissible set of moduli as solutions of Eq. (9) with now

$$b = \mu A' L + K\left(\frac{1}{\mu}\right) \tag{14}$$

and the consequent definition (11) of d. The consistency condition (12) still holds here with the above function b.

Note that in both expressions (8) and (13), the parameter A does represent the maximum value of the amplitude of the solution, reached at $x=0$ for the even states (13) and at $x=K(1/\mu)$ for the odd states (8).

NONLINEAR SPECTRUM

Figure 3 displays the solutions of Eq. (9) for $V=1$ and $L=4$ in the odd and even cases, for which the associated linear problem possesses three eigenstates (dashed lines). The three curves show the dependency of the eigenvalue of each nonlinear extension of the linear levels in terms of the amplitude A. These eigenvalues are given by the expression (6) for each solution μ of Eq. (9), in both cases (10) and (14), equations that are solved numerically (like in the linear case).

Figure 4 shows three examples of linear and nonlinear states corresponding to particular choices of amplitudes and frequencies, as indicated on the graphs. These are the plots of the solutions (8) and (13), compared to the linear eigenfunctions (2) and (3).

There are two fundamental properties of this *"nonlinear spectrum"* apparent in Fig. 3 that we demonstrate hereafter. First, there is the property to reach the linear spectrum for vanishing amplitudes, which explains why we have the same number of states as the linear levels. Second, all three curves are seen to stop at some threshold amplitude which can be exactly computed, as shown by the dashed curve in Fig. 3 and by the crosses which are the predicted thresholds.

LINEAR LIMIT

To demonstrate in general that the nonlinear spectrum goes to the linear one in the limit $A\to 0$, it is crucial to evaluate the limits keeping the product $A\mu$ finite. Actually defining $k=A'\mu$, we easily obtain $(A=A'\sqrt{2})$

$$Asn(\mu A' x, 1/\mu) \underset{A\to 0}{\sim} A\sin(kx), \tag{15}$$

which proves that the nonlinear odd states (8) tend to the linear ones in the limit $A\to 0$. The same property holds naturally for the nonlinear even states (13) by using $\mathrm{sn}(u+K(\nu),\nu)=\mathrm{cd}(u,\nu)$ and $\mathrm{cd}(u,0)=\cos(u)$ together with Eq. (15) above.

These results show in particular that the *"nonlinear wave number"* is the quantity $k=A'\mu$ and thus that the relation (6) must be read $\omega^2=k^2+A^2/2$ that tends to the linear dispersion relation $\omega^2=k^2$ in the small amplitude limit.

NONLINEAR TUNNELING

More interesting is the existence of a threshold amplitude (or population threshold) beyond which gap solitons are emitted outside the well, hence realizing a classical nonlinear tunneling. This is the result of an instability, as described in [13], which takes place as soon as the amplitude A is such that the soliton tail (4) reaches its maximum value in $|x|$

$=L$, i.e., $d=0$. It is worth noting that the nonlinear state solutions hold only for amplitudes A below the threshold; they do not describe the solution after the development of the instability. Such an instability has been recently shown to be at the origin of gap soliton generation in Bragg gratings [14].

In order to derive the analytic expression of the thresholds positions $\{A_s, \omega_s\}$ for each branch $\omega(A)$, we express the continuity conditions in $|x|=L$ in the case $d=0$. The threshold is thus obtained as a particular solution of the equation for the state (9) for which both sides vanish altogether (successively for the odd and even states), namely

$$cn^2\left(b, \frac{1}{\mu}\right) dn^2\left(b, \frac{1}{\mu}\right) = 0, \tag{16}$$

$$\frac{2V}{A^2} - (1+\mu^2) - sn^2\left(b, \frac{1}{\mu}\right) = 0, \tag{17}$$

where b is given by Eq. (10) for the odd solutions and by Eq. (14) for the even ones.

It is then a matter of algebraic manipulations to demonstrate that the solutions $\{A_s, \mu_s\}$ of the above equations globally satisfy

$$A_s^2 = \frac{2V}{2+\mu_s^2} = 2(V-\omega_s), \tag{18}$$

where μ_s is obtained by solving for the odd case

$$sn^2\left(L\mu_s \sqrt{\frac{V}{\mu_s^2+2}}, \frac{1}{\mu_s}\right) = 1, \tag{19}$$

and for the even case

$$sn^2\left(L\mu_s \sqrt{\frac{V}{\mu_s^2+2}} + K\left(\frac{1}{\mu_s}\right), \frac{1}{\mu_s}\right) = 1. \tag{20}$$

Note that the solutions $\{A_s, \mu_s\}$ of these equation must obey requirement (7), which is checked *a posteriori*.

The dashed curve of Fig. 3 is the plot of Eq. (18) for $V=1$ and $L=4$, and the crosses are obtained by solving Eqs. (19) and (20) numerically.

The above procedure does not furnish the threshold corresponding to the fundamental level. Indeed, it misses the particular solution

$$\mu_s = 1, \quad A_s^2 = \frac{2}{3}V, \tag{21}$$

which is effectively a solution of Eqs. (16) and (17) from the property

$$\lim_{\mu \to 1} \left\{ sn\left(a + K\left(\frac{1}{\mu}\right), \frac{1}{\mu}\right) \right\} = 1 \tag{22}$$

for any real-valued a. In that case, the *"dispersion relation"* (6) provides $\omega_s^2 = A_s^2$. Note that the threshold amplitude A_s does not depend on the width $2L$ of the well.

SOLITON GENERATOR

This last solution is particularly interesting in view of applications to our fiber guide array device. Indeed, in that case the corresponding expression (13) is the constant amplitude field $\psi = A_s e^{-i\omega_s t}$.

Injecting then in the medium (as indicated by the arrows in Fig. 1) a CW-laser beam of (normalized) intensity flux A_s^2 constant along the tranverse x direction for $x \in [-L, +L]$, one would generate a gap soliton propagating outside the well, as displayed in Fig. 2. Such simulation can be reproduced *ad libidum* for the input data constant in $[-L, +L]$ and exponentially vanishing outside: as soon as the amplitude exceeds the threshold A_s, one obtains tunneling by soliton emission.

An important issue is the necessity of nonlinearity sign change. When the whole array presents an attractive (focusing) nonlinearity, similar states are defined in terms of Jacobi cn functions [11]. We have observed on numerical simulations that they experience modulational instability largely before reaching the threshold amplitude. In the other case when the whole medium is defocusing, the outside tails are of cosech-type [11], which allows to match any amplitude of the nonlinear state, thus implying overall stability (no threshold and no gap soliton generation) just like in the linear case. The proposed nonlinearity sign change is thus a means for ensuring a threshold for soliton generation and for stabilizing the nonlinear states below the threshold.

PERSPECTIVES AND CONCLUSION

We have so far demonstrated the existence of *"nonlinear eigenstates,"* exact solutions of the NLS model (1), that are remarkably stable (numerical simulations did not show any deviation from the exact expressions up to times when numerical errors become sensible, i.e., 10^3 to 10^4 for our scheme) as soon as their amplitudes do not exceed a threshold explicitly evaluated in terms of the well height for each mode. These states reproduce exactly, in the small-amplitude limit, the usual eigenstates of the Schrödinger equation in a potential well. The approach applies straightforwardly to a model where the inside of the well would obey the linear Schrödinger equation.

At threshold amplitude, a *nonlinear tunneling* (macroscopic, classical) occurs by the emission of gap solitons outside the well. This generic property shows that the proposed fiber guide array resonator will act as a *gap soliton generator* under CW irradiation, and that the ouput signal will switch at threshold amplitude.

Although the present formalism has been developed for continuous envelopes (large number of fiber guides and weak transverse coupling), preliminary numerical simulations of the discrete case do show gap soliton formation. An interesting issue is then the discrete version of the nonlinear states.

In future studies we will explore the important question of the analytical proof of the stability of those states, including the mathematical derivation of the instability criterion at threshold amplitude. Note finally that, in the threshold regions, the states are degenerated: two solutions coexist at the same frequency with slightly different amplitudes, as seen in Fig. 3.

[1] A. Yariv, *Optical Electronics*, 4th ed. (Saunders College Press, Orlando, FL, 1991).
[2] T. Pertsch, T. Zentgraf, U. Peschel, A. Brauer, and F. Lederer, Phys. Rev. Lett. **88**, 093901 (2002).
[3] D.N. Christodoulides and R.I. Joseph, Opt. Lett. **13**, 794 (1988).
[4] R. Morandotti, H.S. Eisenberg, Y. Silberberg, M. Sorel, and J.S. Aitchison, Phys. Rev. Lett. **86**, 3296 (2001).
[5] D. Mandelik, H.S. Eisenberg, Y. Silberberg, R. Morandotti, and J.S. Aitchison, Phys. Rev. Lett. **90**, 053902 (2003).
[6] D. Mandelik, R. Morandotti, J.S. Aitchison, and Y. Silberberg, Phys. Rev. Lett. **92**, 093904 (2004).
[7] A.A. Sukhorukov, D. Neshev, W. Krolikowski, and Y.S. Kivshar, Phys. Rev. Lett. **92**, 093901 (2004).
[8] R. Khomeriki, Phys. Rev. Lett. **92**, 063905 (2004).
[9] F. Geniet and J. Leon, Phys. Rev. Lett. **89**, 134102 (2002); J. Phys.: Condens. Matter **15**, 2933 (2003).
[10] Y.S. Kivshar and G.P. Agrawall, *Optical Solitons: From Fibers to Photonic Crystals* (Academic Press, San Diego, CA, 2003).
[11] L.D. Carr, K.W. Mahmud, and W.P. Reinhardt, Phys. Rev. A **64**, 033603 (2001).
[12] L.D. Carr, C.W. Clark, and W.P. Reinhardt, Phys. Rev. A **62**, 063610 (2000); **62**, 063611 (2000).
[13] J. Leon, Phys. Lett. A **319**, 130 (2003).
[14] J. Leon and A. Spire, Phys. Lett. A **327**, 474 (2004).